catalysts

MDPI

Article

Impregnation Protocols on Alumina Beads for Controlling the Preparation of Supported Metal Catalysts

Alejandra C. Bueno [1,2], Maxime Mayer [2], Matthieu Weber [3], Mikhael Bechelany [3], Michaela Klotz [2] and David Farrusseng [1,*]

[1] Ircelyon, UMR 5256 CNRS, Univ. Lyon 1, 2 av. Albert Einstein, 69100 Villeurbanne, France
[2] LSFC UMR 3080 CNRS / Saint-Gobain CREE, Saint-Gobain Research Provence, 550 avenue Alphonse Jauffret, Cavaillon, France
[3] IEM, UMR5635 ENSCM, CNRS, Univ. Montpellier, Place Eugène Bataillon, 34095 Montpellier, France
* Correspondence: david.farrusseng@ircelyon.univ-lyon1.fr

Received: 28 May 2019; Accepted: 24 June 2019; Published: 30 June 2019

Abstract: Whereas the synthesis principles of supported metal catalysts are well documented in the open literature, impregnation protocols on shaped bodies represent sensitive industrial know-how and are, therefore, rarely found. We investigated various synthesis parameters for both wetness (WI) and dry (DI) impregnations to prepare Pd/γ–Al_2O_3 alumina beads. Two kinds of catalysts were achieved: homogeneously dispersed catalysts with no metal gradient across the beads and eggshell catalysts. A combination of optical images, Castaing microprobe analysis, elemental analysis, and TEM made it possible to discriminate between catalysts according to their metal loading, location across the bead diameter, and metal dispersion. Regardless of the macropore structure of the alumina beads, we found that volatile solvents (acetone) were preferred for preparing homogeneous catalysts by WI, whereas the use of a viscous aqueous solution (water/glycerol) in DI resulted in an eggshell-type catalyst. The atomic layer deposition (ALD) method was also investigated as a physical vapor phase deposition method for preparing eggshell catalysts. Representative-shaped catalysts were tested for CO oxidation as a model reaction in order to highlight the differences between catalysts with a homogeneous metal distribution (no metal gradient) and eggshell-type.

Keywords: impregnation; catalyst support; catalyst carrier; eggshell catalyst; homogeneously dispersed catalyst

1. Introduction

The size and shape of catalyst carriers are a trade-off between the desire to minimize pore diffusion effects in the catalyst bodies while also the pressure drop across the reactor. Shaped bodies include pellets, extrudates, beads, or more complex forms such as trilobes and monoliths. It is well known that it is important to control the impregnation profile for pre-shaped supports when preparing commercial catalysts [1]. The location of the metal throughout the support is a key parameter in determining catalyst effectiveness, i.e., the portion of the catalyst that is actually working under reaction [2]. For reactions with high intrinsic activities, a gradient of metal concentration will be desired, as in an eggshell configuration, in order to reduce the content of unused metal, and therefore, reduce the price of the catalyst. In contrast, for "slow" reactions, a homogeneous location of the metal particles in the support body will be preferred [3].

Whereas the synthesis principles of supported metal catalysts are well documented in the open literature, impregnation protocols on shaped bodies represent sensitive industrial know-how and are, therefore, rarely found [4–6]. Supported catalysts are often applied because they combine a relatively high dispersion (amount of active surface metal) with a high degree of thermostability [7].

These catalysts are made involving a sequence of several complex processes, typically by impregnation of the porous support with a solution containing a precursor, the choice of which is crucial for the final dispersion. It is followed by drying to remove the excess solvent, heating in air and reduction of the metal. Slight variations during the preparation may result in critical alteration in the properties of the final catalyst. Based on previous reports and model calculations, many researchers such as Morbidelli et al. [8] and Schwarz and Heise [9], concluded that several experimental factors but also from physical/chemical nature, may cause critical heterogeneities in the preparation of supported metal catalysts. Some of these are, for example, the components of the solution, pH, temperature, ionic strength, the support-metal interaction, and the competition with precursor species for the same adsorption sites and drying conditions.

For industrial-scale millimeter-sized support bodies, non-uniform metal loadings such as eggshell, egg yolk, or egg white are generally sought [10,11]. Iglesia and coworkers [12] proposed an alternative route to synthesize eggshell catalysts by controlling the rate of diffusion of the metal salt solution into the support. Recently, it was pointed out that eggshell catalysts can be produced during the drying process depending on the relative importance of adsorption, diffusion, and convection during the drying process [13], and the thickness of the core can be controlled by varying the evaporation time of the organic solvent.

The aim of this work was to optimize preparation techniques for the control of the distribution of metal in alumina beads in view of obtaining eggshell catalysts and homogeneous catalysts. Two types of γ-Al_2O_3 beads of mm diameter with similar textural properties but distinct pore structures were investigated. The preparation methods investigated here are the classic techniques of wet impregnation (WI) and dry impregnation (DI). In addition, atomic layer deposition (ALD) was also studied as a new potential deposition technique for shaped supports [14,15]. Relevant and representative optimized catalysts were tested for CO oxidation as a model reaction [16].

2. Results and Discussion

The two catalyst supports investigated only differed in their macropore connectivity. The first support, obtained from Sasol, has spherical and micrometer-sized macropores. It will be referred to as "CP"—standing for "closed macropores"—because the macropores communicate only through the mesopores. The second support, obtained from Norpro, had interconnected, randomly dispersed macropores, and will be referred to as "RP." Both supports were impregnated by 0.2 wt.% Pd composing the catalysts, following the impregnation protocols investigated.

First of all, visual inspection is an easy and efficient way to evaluate where the metal is deposited. After metal salt impregnation, the supports turned yellowish and appeared to be homogeneous. Upon reduction of the Pd to metal during the post-treatment, the catalysts turned a typical brown color, but in different tones. As suggested by Poncelet et al. [17], the intensity of the color of the support can be related to the amount of metal adsorbed, although it is not quantitative.

The impregnation of the homogeneously dispersed catalysts by WI requires that the metal salt solution is added in excess of the pore volume of the support. The catalysts impregnated by WI (CP-WI-Ea in Figure 1B) were homogeneous in color, which is likely explained by a homogeneous dispersion of the metal in the final catalyst. For DI, the catalysts in Figure 1A,C,E seemed heterogeneous. The preparation by DI requires that the volume of solution is either equal to or less than the porous volume of the support, which may result in a higher metal concentration, possibly leading to precipitation. Interestingly, however, the use of acetone as the solvent permitted better homogeneity (Figure 1D,F) of color than did ethanol, even when, for both cases, the inside of the beads was colored. The drying step is crucial and usually results in severe redistribution of the impregnated species [9,18,19]. Although acetone and ethanol are of similar viscosity (0.3 mPa·s) [20,21], ethanol has a lower surface tension. Capillary forces are key parameters that may control the homogeneity of the preparation when the solvent is removed upon drying. Thus, we can assume that because acetone evaporates faster than ethanol due to the higher volatility and surface tension, it is more favorable for a homogeneous dispersion of the particles.

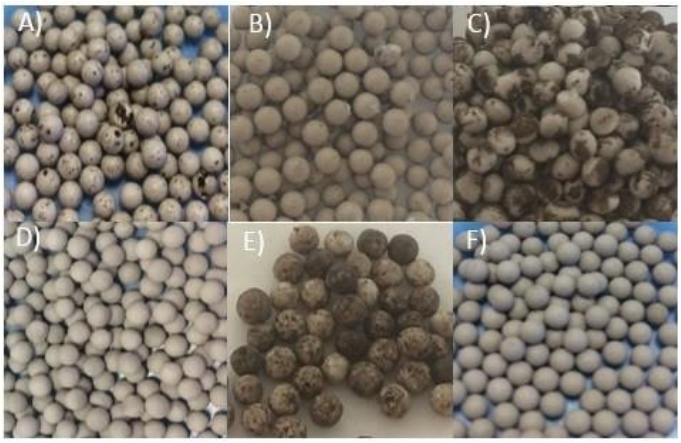

Figure 1. Appearance of the homogeneously dispersed catalysts: **A**) CP-DI-Ea, **B**) CP-WI-Ea, **C**) RP-DI-Ec, **D**) CP-DI-Ab, **E**) RP-DI-Aa, and **F**) RP-DI-Ab.

Obtaining eggshell catalysts by DI involved the use of a viscous solvent. Following DI, a mixture of water and glycerol was used to prevent a deep penetration of the Pd within the beads. However, some catalysts were heterogeneous in color. As already mentioned, the solubility of the precursor in the solution is a crucial factor, so that the concentration profile of the precursor on the support surface depends significantly on the conditions during the first steps of the preparation. For instance, $Pd(C_5H_8O_2)_2$ could not be dissolved into glycerol, unlike $Pd(NO_3)_2$. Regarding the solvents, two different ways of preparing the metal salt solution were investigated, in view of dissolving the metal precursor as thoroughly as possible in the water–glycerol mixture. Thus, the viscosity of glycerol prevents complete solubility when the solution is prepared simultaneously (DI-1). In contrast, by first dissolving the metal precursor in water and then adding the glycerol (DI-2), high solubility can be achieved, resulting in homogeneously colored catalysts (see Figure 2C). Atomic layer deposition resulted in perfectly homogeneous brown beads that were slightly darker than the other catalysts. Fracturing the beads in half showed that the metal did not penetrate within the support with the conditions used for this ALD deposition (Figure 2D).

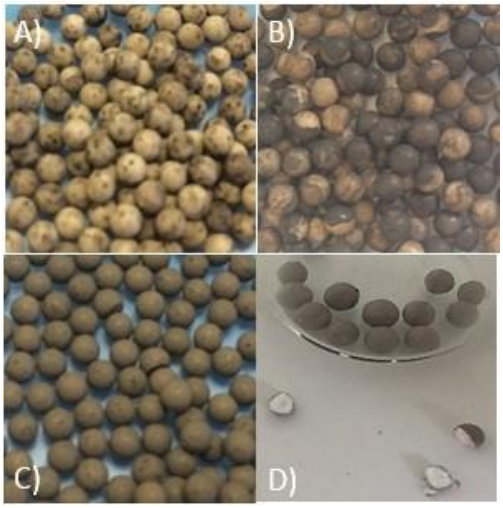

Figure 2. Appearance of the eggshell catalysts: **A**) CP-DI-C1, **B**) CP-DI-N1, **C**) CP-DI-N2, and **D**) RP-ALD.

For a quantitative approach, the Pd location within selected supported metal beads was examined using Castaing microprobe analysis on a bead section. Diverse Pd cartographies were acquired for the various catalysts, with an analyzed zone of 1.5 × 1.5 mm², and 400 × 400 µm² to highlight the presence of palladium. The color scale was arbitrarily chosen to make the small differences noticeable, as the content per bead was very low. Figure 3 shows the Pd distribution obtained following the protocols investigated for the preparation with homogeneous dispersion. The catalyst impregnated using acetone showed a better homogeneous dispersion of Pd. On the contrary, the use of ethanol resulted in catalysts with a higher concentration of Pd at the edges, likely due to the lower solubility previously mentioned. These catalysts could neither be considered as eggshell nor as homogeneously dispersed. Furthermore, one can observe a slightly different microstructure at the edges of the CP-catalysts, which seemed darker compared to the rest of the bead. This may result from the fact that this support was denser within 5 µm at the edges (see Figure A1 in Appendix). The analysis of this section showed an increased presence of C and Cl from the resin, and thus, a darker halo of chemical contrast was observed. Comparison of the DI protocols indicated that the process of introducing the beads continuously into a vial (protocol b) rather than into the opened container (protocol a) could contribute to better stability of the conditions during impregnation overnight. On the contrary, the beads on the Petri dish (protocol c) did not benefit from rotation for homogenizing the metal solution over the beads.

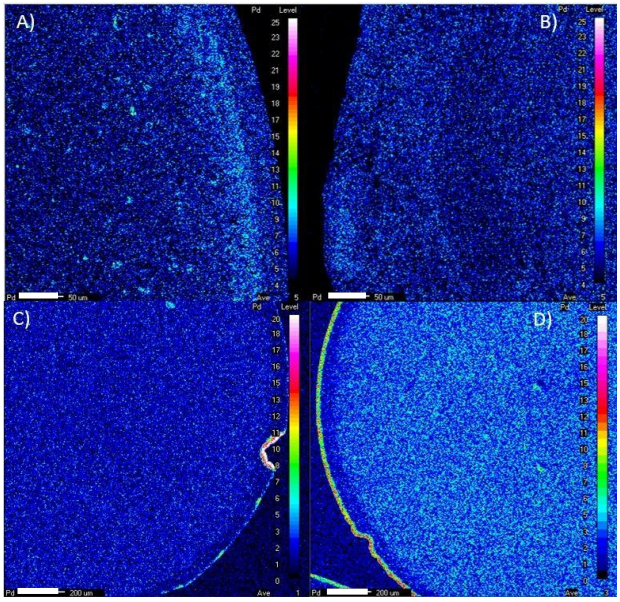

Figure 3. Microprobe cartographies of Pd on the homogeneously dispersed catalysts: **A**) CP-DI-Ab, **B**) RP-DI-Ab, scale bar = 50 μm, **C**) CP-DI-Ea, and **D**) CP-DI-Ec, scale bar = 200 μm.

The cartographies of the eggshell catalysts impregnated using protocols DI-b and ALD are shown in Figure 4 A–C and B–D, respectively. The metal shells showed different thicknesses depending on the penetration of the metal within the support. The Pd thickness was more regular for the CP support than for the RP, due to its random porosity. For instance, while the Pd shell of the CP-DI-N2 measured 33 μm, for that of the CP-ALD it was reduced by half. For the RP support, the Pd shell impregnated by DI had an approximate thickness of 60 μm, which was significantly higher than that of the CP support impregnated using the same protocol. Interestingly, using ALD, the same thickness of 16 μm was observed for both supports, regardless of the porosity of the support.

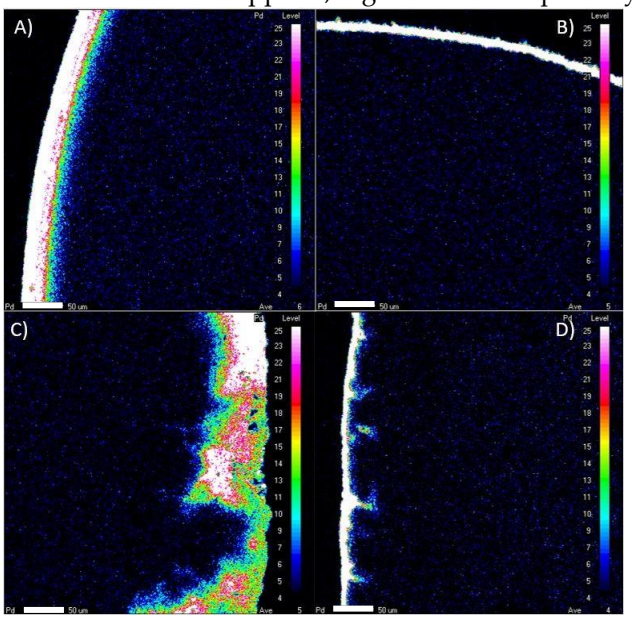

Figure 4. Microprobe cartographies of Pd on the eggshell catalysts: **A**) CP-DI-N2, **B**) CP-ALD, **C**) RP-DI-N2, and **D**) RP-ALD. Scale bar = 50 μm.

In order to rule out measurement bias or sample preparation effects (resins), WDS qualitative analysis on the edge, center, and core were carried out on homogeneously and eggshell dispersed catalysts. Figure 5 shows these analysis for RP-DI-Ab and RP-DI-N2 as examples of both types of catalysts. The signals of Pd were characterized by the peaks of Lβ1 at 0.414 nm and Lα1 at 0.437 nm. Thus, it can be confirmed that the Pd was present in the three areas for the homogeneously dispersed catalyst. On the other hand, the eggshell catalyst only showed the Pd peaks at the edge of the bead. They can have different intensities depending on its quantity within the support (see Table 1). Quantitative analysis was not be considered, due to the presence of an interaction of the Kβ line of Cl at 0.44 nm with the Lα1 line of Pd, which distorts the results.

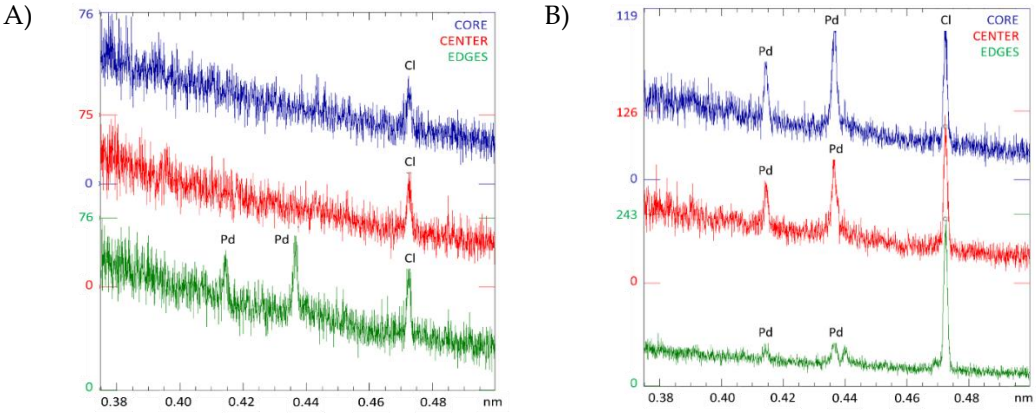

Figure 5. Qualitative microprobe analysis on 20 × 20 μm² of **A**) CP-DI-N2 as eggshell catalyst and **B**) RP-DI-Ab as homogeneously dispersed catalyst.

Although the amount of Pd in the precursor solution should have been enough to obtain catalysts with a metal content of 0.2 wt.% Pd, we can see that the loading obtained varied from protocol to protocol. Under equilibrium conditions, the amount introduced into the beads depends on the equilibrium concentration of the impregnating solution, the pore volume of the support, and the adsorption isotherm that describes the binding of the precursor onto the support surface [22]. According to the following results, the Pd content of the catalysts impregnated by WI was very low. As mentioned before, some of the Pd concentration could remain outside of the beads. However, increasing the weight loading, by adding some extra milligrams of metal precursor during impregnation, requires higher concentrations that may cause substitution of ions into the support lattice, thereby disrupting the support, as already investigated by Driscoll et al. [23]. In addition, an important question following the DI technique is if all pores were effectively filled with the precursor solution. The use of a volume of impregnation solution that equals the pore volume prevents the capillary forces from driving the uptake of the solution into the support to the last drop of precursor solution [24]. It can concurrently be observed that with acetone, the homogeneous catalysts also present a higher amount of Pd than do the catalysts impregnated with ethanol. The eggshell catalyst impregnated by $Pd(C_5H_8O_2)_2$ and water/glycerol, CP-DI-C2, have a lower content of Pd due to the insolubility of the precursor in glycerol. Again, the simultaneous mixing of the solvents in DI-2 led not only to inaccuracy but also to heterogeneous coloring of the catalyst. Though $Pd(NO_3)_2$ was soluble, the desired metal content was achieved only by the DI-2 method in this case.

Table 1. Pd content of the catalysts by ICP analysis ([a] see Table 2 for the catalyst name).

Catalyst [a]	wt. % Pd
CP-WI-Ea	0.04
CP-DI-Ea	0.06
RP-DI-Eb	0.07
CP-DI-Ab	0.19
RP-DI-Ab	0.2
RP-DI-Aa	0.16
CP-DI-C1	0.03
RP-DI-N1	0.07
CP-DI-N2	0.2
RP-DI-N2	0.2
CP-ALD	0.28
RP-ALD	0.12

The TEM analysis was carried out on the homogeneous catalysts to determine the mean diameter of the metal particles. Spherical Pd particles with a mean diameter of 2–3 nm were measured for the homogeneous catalysts RP-DI-Ab and CP-DI-Ab, corresponding to a metal dispersion (percentage of metal atoms at the surface of the metal particles) of 29% and 34%, respectively. The particle size of the eggshell catalysts (DI-b and ALD protocols) could not be measured by TEM neither by CO chemisorption due to the very low Pd amount.

Figure 6 shows typical "light-off" plots of CO oxidation for the catalytic activity of CP-ALD as a representative eggshell catalyst, and CP-DI-Ab as a representative homogeneous catalyst. The catalytic activities of the supported Pd beads were compared with the corresponding CP-DI-Ab powder after grinding and sieving at 300 μm, and were expressed per gram of Pd as a function of temperature. The temperature profile activities for a rise–descent cycle from room temperature to 350 °C of the three catalysts were typical of light-off phenomena occurring at about 150 °C. The activity plateaus corresponded to 100% CO conversion. The activity at 100% conversion was lower for the ALD-made catalysts, likely because of their larger Pd particles. By comparing the homogeneous catalyst and its corresponding powder, it can be seen that the activities at low temperature (below

170 °C) and at high temperature (beyond 225 °C) were exactly the same. The activity of the catalytic beads increased at a lower rate when conversion was higher than 20%. This is a typical indication of transport-limited phenomena that result in partial use of the bead volume (effectiveness), i.e., available metal. In the powder, such transport limitation does not occur, because the grain diameter is 1 μm as opposed to 2.5 and 3 mm for the beads. On the contrary, for the eggshell catalysts, we observed a very steep light-off similar to the powder. This light-off profile was expected, as the Pd particles were mostly located at the external surface of the support, resulting in negligible internal mass transport. Finally, having characterized the light-off profiles of catalytic powder and an eggshell-type catalyst, we can assume that the smoother light-off profile observed for the DI-made catalyst corresponds to an effective homogeneity of the metal particle location throughout the beads.

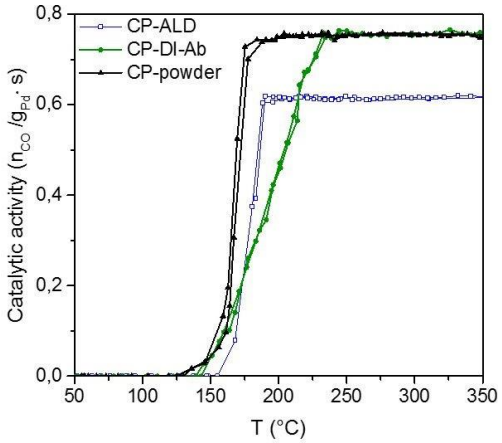

Figure 6. Catalytic activities in CO oxidation of CP-ALD as eggshell catalyst, CP-DI-Ab as homogeneous catalyst, and its corresponding powder. Rise and descent from room temperature to 350°C.

3. Materials and Methods

The textural properties of both supports, assessed using nitrogen adsorption and mercury intrusion porosimetry (Table 2), were very similar.

Table 2. Textural analysis of the catalyst supports, where [a] means assessed by nitrogen sorption and [b] by mercury intrusion porosimetry.

Support	$D_{,bead}$ (mm)	$SSA_{,BET}$ [a] (m^2/g)	$Dp_{,BJH}$ [a] (nm)	Vp [b] (cm^3/g)	$\varrho_{,apparent}$ [b] (g/cm^3)	Porosity [b] (%)
CP	2.5	198	10	0.7	3.1	67
RP	2.8	197	11	0.8	3.1	66

The impregnation techniques investigated are described below. A summary of all catalysts and their preparation protocols is given below in Table 3.

Table 3. Summary of the impregnation techniques studied and the catalyst prepared.

Metal Location	Impregnation Technique	Precursor	Solvent	Method	Catalyst Name
Homogeneously dispersed	Wet Impregnation (WI)	$Pd(C_5H_8O_2)_2$	ethanol	a	RP-WI-Ea
					CP-WI-Ea
			acetone	a	RP-DI-Aa

	Dry impregnation (DI)			b	RP-DI-Ab
					CP-DI-Ab
			ethanol	a	CP-DI-Ea
				b	RP-DI-Eb
				c	RP-DI-Ec
Eggshell	Dry impregnation (DI)	$Pd(C_5H_8O_2)_2$	H_2O + glycerol	a-1	CP-DI-C1
			H_2O/glycerol	a-2	CP-DI-C2
		$Pd(NO_3)_2{\cdot}H_2O$	H_2O + glycerol	a-1	CP-DI-N1
			H_2O + glycerol	a-2	CP-DI-N2
					RP-DI-N2
	Atomaic layer deposition (ALD)	$Pd(hfac)_2$	-	-	CP-ALD
					RP-ALD

3.1. Homogeneously Dispersed Catalysts

Wet impregnation (WI) and dry impregnation (DI, also called incipient wetness impregnation) techniques were investigated under different protocols. These techniques were performed for 1–2 g of beads at a time. Palladium(II) acetylacetonate, $Pd(C_5H_8O_2)_2$, (Strem Chemicals, 99%) was used as the Pd precursor. Regarding the solvents, both acetone (99%) and ethanol (95% denatured) were used. While for the WI, the different metal salt solutions were used in excess of 40% by volume, for DI the volume of solution was equal to the pore volume, Vp, for the mass of beads to impregnate. It was calculated using the Vp obtained by mercury intrusion porosimetry (see Table 2). Diverse methods were investigated:

- Method WI-a: A polyoxymethylene-based container was built to hold the beads. It has a cylindrical shape with convex internal borders, and measured 5 cm and 6.2 cm in internal and external diameter, respectively. It also had an external connection to be placed into a turned-around overhead stirrer (Bioblock Heidolph). The assembly simulated a cement mixer, without paddles, secured in place by a laboratory stand. The beads were placed inside the container at 45° and turned at 3 rpm. The prepared metal salt solution was poured over the beads. The container was then covered by a paraffin film, and turned under mechanical rotation overnight.
- Method DI-a: same method as for WI-a.
- Method DI-b: The beads were introduced into a vial in which the prepared metal salt solution was then added. The ensemble was deposited onto a tube roller mixer (RSLAB-10 Rogo-Sampaic). It turned overnight at 30 rpm under mechanical rotation.
- Method DI-c: The beads were placed in a monolayer on a Petri dish, and the metal salt solution was added dropwise over the beads. It was observed that each bead could absorb 2–3 drops. Then, the beads were dried at 60 °C overnight in a forced-air oven, and followed the post-treatment indicated below.

3.2. Eggshell catalysts

Two preparation techniques were investigated following the DI-a method and by atomic layer deposition (ALD).

Following DI-a, two metal salt solutions were prepared in a 0.8 deionized H_2O/0.2 glycerol (Sigma–Aldrich, 99%) volume ratio using $Pd(C_5H_8O_2)_2$ or palladium(II) nitrate hydrate, $Pd(NO_3)_2$ xH_2O (Strem Chemicals, 99.9%-Pd) as metal precursors. Regarding the solvent used to dissolve the metal salts, two methods were investigated. In method a-1, the Pd precursor was dissolved simultaneously in an H_2O + glycerol mixture, whereas in method a-2, the metal salt was first

dissolved in water, and then the glycerol was added. Once the metal solution was prepared, it was poured over the beads into a vial. The impregnation lasted 15 min.

Regarding ALD, 300 ALD cycles were applied in a low-pressure hot-wall (home-built) ALD reactor. The ALD process was based on sequential pulses of palladium(hexafluoroacetylacetonate)$_2$ (or Pd(hfac)$_2$) and formalin precursors (both were purchased from Sigma–Aldrich). Briefly, the ALD cycle consisted of a 0.5 s pulse of Pd(hfac)$_2$, 15 s of exposure, and a 10 s Ar purge, followed by a 1 s pulse of formalin, 15 s of exposure, and again a 15 s purge with Ar. The bubbler containing the Pd(hfac)$_2$ precursor was heated to 70 °C to provide sufficient vapor pressure, and the formalin container was kept at room temperature. The vacuum chamber was set at a temperature of 220 °C, and the lines were heated at 100 °C in order to prevent condensation. Further details about both this deposition protocol and the associated ALD reactor can be found elsewhere [25,26].

3.3. Post-Impregnation Treatment

All catalysts needed pre-treatment after impregnation, except those prepared by ALD, which were reduced in situ. The beads were dried in a rotatory evaporator at 50 °C followed calcination by thermal treatment under 100 ml/min of O_2. The final temperature depended on the metal precursors: 350 °C for $Pd(C_5H_8O_2)_2$, and up to 550 °C for impregnations performed with $Pd(NO_3)_2$ xH_2O. The heating rate was 1 °C/min in both cases, followed by a 2 h plateau. The reduction of the active phase was then performed under 100 mL/min of H_2 at 500 °C (1 °C/min), with a 2 h plateau.

3.4. Characterization Methodology

N2 sorption measurements were carried out on entire beads at the boiling point of nitrogen (77 K) using a Belsorp-mini II Japan INC apparatus. The beads were previously outgassed at 350 °C under vacuum for 3 h using a Belprep II Japan INC instrument. Specific surface area calculations were performed using the BET method [27] and the pore size distribution was evaluated using the BJH method [28]. Mercury intrusion porosimetry measurements were also performed on entire beads using a Micromeritics AutoPore IV 9500 apparatus. The pressure was graduated from 45 to 30,000 psi. Elemental analysis by ICP was recorded using an Activa Horiba spectrometer. A Castaing microprobe analysis was performed using a Hyprobe JEOL JXA8530F coupled with 4 wavelength dispersive X-ray (WDS) JEOL spectroscopes on resin embedded and polished samples. The metal dispersion was defined as the ratio between the number of surface metal atoms and the total number of metal atoms. Assuming face-centered cubic (fcc) palladium, the dispersion D can be expressed as [29]:

$$D = 1.12/ds, \quad (1)$$

$$ds = \sum_{i=1}^{n}(n_i \cdot d_i^3)/\sum_{i=1}^{n}(n_i \cdot d_i^2) \quad (2)$$

where d_s corresponds to the Sauter diameter. For each particle n_i, the diameter di, expressed in nanometers, was determined on TEM images assuming a spherical shape. Five hundred Pd particles were measured for the calculation. TEM (JEOL 2100F) analysis was performed by preparing the samples by replica: the alumina matrix was attacked by an HF treatment, making it possible to observe only metal particles on the TEM grids.

4. Conclusions

We have shown that, in many cases, impregnation protocols led to severe heterogeneity in metal loading location and dispersion for shaped catalysts. We found that for dry impregnation using a tube roller mixer, $Pd(C_5H_8O_2)_2$ and acetone led to optimal metal homogeneity across the bead diameter. The light-off profile in CO oxidation showed a transport-limited regime, which is in line with a homogenous location of metal throughout the catalytic bead. For the preparation of eggshell catalysts by dry impregnation, a mixture of 0.8 H_2O/0.2 glycerol provided the best results by preventing the penetration of the active phase into the beads. Here, the steep light-off profile for CO oxidation, which is similar to that of the powder, supports the availability of all metal sites. A

technical and economic analysis of the preparation processes at the industrial scale was beyond the scope of this study. In addition to optimizing distinct impregnation methodologies for homogenous catalysts and eggshell catalysts, we have highlighted key physico-chemical parameters of the solvents in order to facilitate rational approaches for controlling the loading of metal particles in shaped bodies. Surprisingly, we found that the macropore texture of the supports was not a determining factor.

Author Contributions: A.C.B., D.F. and M.K. designed the research. A.C.B. performed the experimental work. M.W. and M.B. performed the ALD experiment, M.M. performed the microprobe analysis. All authors analyzed and discussed the results. A.C.B., D.F. and M.K. wrote the paper.

Funding: This research received no external funding.

Acknowledgments: The authors thank Sasol and Saint-Gobain Norpro for providing the beads allowing this study.

Conflicts of Interest: The authors declare no conflict of interest.

Appendix

The following Figure A1 corresponds to SEM images of both supports, CP and RP, using a FEI Nova NanoSem 230. For that, the samples were deposited on a carbon tape and metallized (Cressington Sputter Coater 203HR) under a vacuum of argon by a plasma of Pt. Both images were taken on fractured beads to observe the internal porosity.

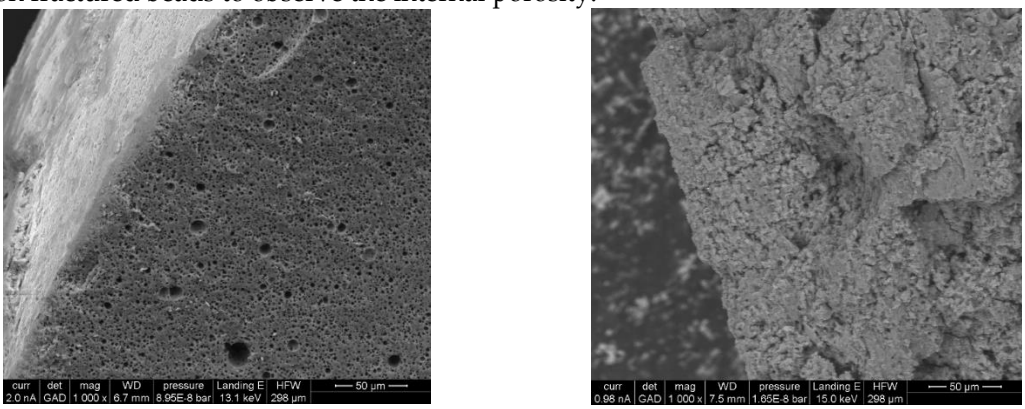

(a) (b)

Figure A1. SEM images of the (**a**) CP-support and (**b**) RP-support. Both beads were fractured in half to observe the internal porosity.

References

1. Komiyama, M. Design and preparation of impregnated catalysts. *Catal. Rev. Sci. Eng.* **1985**, *27*, 341–372.
2. Kalz, K.F.; Kraehnert, R.; Dvoyashkin, M.; Dittmeyer, R.; Glaser, R.; Grunwaldt, J.D. Future Challenges in Heterogeneous Catalysis: Understanding Catalysts under Dynamic Reaction Conditions. *ChemCatChem* **2017**, *9*, 17–29.
3. Munnik, P.; de Jongh, P.E.; de Jong, K.P. Recent Developments in the Synthesis of Supported Catalysts. *Chem. Rev*. **2015**, *115*, 6687−6718.
4. White, R.J.; Luque, R.; Budarin, V.L.; Clark, J.H.; Macquarrie, D.J. Supported metal nanoparticles on porous materials. Methods and applications. *Chem. Soc. Rev*. **2009**, *38*, 481–494.
5. de Jong, K.P. *Synthesis of Solid Catalysts*; Wiley-VCH: Weinheim, Germany, 2009.
6. Plessers, E.; van den Reijen, J.E.; de Jongh, P.E.; de Jong, K.P.; Roeffaers, M.B. Origin and Abatement of Heterogeneity at the Support Granule Scale of Silver on Silica Catalysts. *ChemCatChem* **2017**, *9*, 4562–4569.
7. Perego, C.; Villa, P. Catalyst preparation methods. *Catal. Today* **1997**, *34*, 281–305.
8. Morbidelli, A.; Gavriilidis, A.; Varma, A. *Catalyst Design: Optimal Distribution of Catalyst in Pellets, Reactors, and Membranes*; Cambridge University Press: Cambridge, UK, 2001.
9. Schwarz, J.A.; Heise, M.S. Preparation of Metal Distributions within Catalyst Supports. *J. Colloid Interface Sci*. **1990**, *135*, 461–467.

10. Plessers, E.; Stassen, I.; Sree, S.P.; Janssen, K.P.F.; Yuan, H.; Martens, J.; Hofkens, J.; De Vos, D.; Roeffaers, M.B.J. Rationalizing Acid Zeolite Performance on the Nanoscale by Correlative Fluorescence and Electron Microscopy. *ACS Catal*. **2015**, *5*, 6690–6695.
11. Liu, X.; Khinast, J.G.; Glasser, B.J. Drying of supported catalysts for low melting point precursors: Impact of metal loading and drying methods on the metal distribution *Chem. Eng. Sci*. **2012**, *79*, 187–199.
12. Iglesia, E.; Soled, S.L.; Baumgartner, J.E.; Reyes, S.C. Synthesis and catalytic properties of eggshell cobalt catalysts for the Fischer-Tropsch synthesis. *J. Catal*. **1995**, *153*, 108–122.
13. Lekhal, A.B.; Glasser, J.B.; Khinast, J.G. Impact of drying on the catalyst profile in supported impregnation catalysts. *Chem. Eng. Sci*. **2001**, *56*, 4473–4487.
14. Ritala, M.; Kukli, K.; Rahtu, A.; Räisänen, P.I.; Leskelä, M.; Sajavaara, T.; Keinonen, J. Atomic layer deposition of oxide thin films with metal alkoxides as oxygen sources. *Science* **2000**, *288*, 319–321.
15. Weber, M.; Collot, P.; El Gaddari, H.; Tingry, S.; Bechelany, M.; Holade, Y. Enhanced Catalytic Glycerol Oxidation Activity Enabled by Activated-Carbon-Supported Palladium Catalysts Prepared through Atomic Layer Deposition. *ChemElectroChem* **2018**, *5*, 743–747.
16. Aleksey, A.; Vedyagin, A.A.; Alexander, M.; Volodin, A.M.; Noskov, A.S. Characterization of active sites of Pd/Al_2O_3 model catalysts with low Pd content by luminescence, EPR and ethane hydrogenolysis. *Appl. Catal. B Environ.* **2011**, *103*, 397–403.
17. Zazhigalov, V.A.; Komashko, G.A.; Pyatniskaya, A.I.; Belousov, V.M.; Stoch, J.; Haber, J. Synthesis of VPO Catalysts for Oxidation of C4 Hydrocarbons. In *Studies in Surface Science and Catalysis*; Elsevier: Amsterdam, The Netherlands, 1991; pp. 497–506.
18. Heise, M.S.; Schwarz, J.A. In Preparation of Catalysts IV. Eds. In *Studies in Surface Science and Catalysis*; Elsevier: Amsterdam, The Netherlands; 1987; pp. 1–13.
19. Prieto, G.; Friedrich, H.; de Jong, K.P.; de Jongh, P.E.; Zecevic, J. Towards stable catalysts by controlling collective properties of supported metal nanoparticles. *Nat. Mater.* **2012**, *12*, 34.
20. Rusanov, A.I.; Levichev, S.A.; Tyushin, V.Y.: Composition of the Surface Layer in the n-Hexane-Acetone System. *Vestn. Leningr. Univ*. **1966**, 121–127
21. Vazquez, G.; Alvarez, E.; Nav.za, J.M. Surface Tension of Alcohol + Water from 20 to 50 °C *J. Chem. Eng*. **1995**, *40*, 611–614.
22. Rob van Veen, J.A.; Jonkers, G.; Hesselink, W.H. Interaction of transition-metal acetylacetonates with γ-Al_2O_3 surfaces. *J. Chem. Soc. Faraday Trans.* **1989**, *85*, 389–413.
23. Tsai, W.; Schwarz, J.A.; Driscoll, C.T. Differential cation exchange capacity (DCEC) of nickel supported on silica-aluminas. *J. Catal*. **1982**, *78*, 88–95.
24. Tonetto, G.M.; Damiani, D.E. Influence of the Preparation Method and Metal Precursor Compound on.Alumina-Supported Pd Catalysts, *Int. J. Chem. React. Eng*. **2004**, doi:10.2202/1542-6580.1134.
25. Weber, M.; Kim, J.Y.; Lee, J.H.; Kim, J.H.; Iatsunskyi, I.; Coy, E.; Miele, P.; Bechelany, M.; Kim, S.S. Highly efficient hydrogen sensors based on Pd nanoparticles supported on boron nitride coated ZnO nanowires, *J. Mater. Chem. A* **2019**, *7*, 8107–8116.
26. Weber, M.; Kim, J.H.; Lee, J.H.; Kim, J.Y.; Iatsunskyi, I.; Coy, E.; Drobek, M.; Julbe, A.; Bechelany, M.; Kim, S.S. High-Performance Nanowire Hydrogen Sensors by Exploiting the Synergistic Effect of Pd Nanoparticles and Metal-Organic Framework Membranes, *ACS Appl. Mater. Interfaces* **2018**, *10*, 34765–34773.
27. Brunauer, S.; Emmett, P.H.; Teller, E. Adsorption of gases in multimolecular layers. *J. Am. Chem. Soc*. **1938**, *60*, 309–319.
28. Barrett, E.P.; Joyner, L.G.; Halenda, P.P. The determination of pore volume and area distributions in porous substances. I. Computations from nitrogen isotherms. *J. Am. Chem. Soc.* **1951**, *73*, 373–380.
29. Van Hardeveld, R.; Hartog, F. The statistics of surface atoms and surface sites on metal crystals. *Surf. Sci*. **1969**, *15*, 189–230.

.